BIOMOLECULES & THERAPEUTICS

Original Article
Biomol Ther 32(5), 640-646 (2024)

Glycogen Phosphorylase Inhibitor Promotes Hair Growth via Protecting from Oxidative-Stress and Regulating Glycogen Breakdown in Human Hair follicles

Bomi Park[1,†], Daeun Kim[1,†], Hairu Zhao[1], SoonRe Kim[2], Byung Cheol Park[2,3], Sanghwa Lee[4], Yurim Lee[4], Hee Dong Park[4], Dongchul Lim[4], Sunyoung Ryu[1] and Jae Sung Hwang[1,*]

[1]Department of Genetics & Biotechnology, Graduate School of Biotechnology, College of Life Sciences, Kyung Hee University, Youngin 17104,
[2]Basic and clinical Hair institute, Dankook University, Cheonan 31116,
[3]Department of Dermatology, Dankook University Hospital, Cheonan 31116,
[4]Innovo Therapeutics Inc., Seoul 04174, Republic of Korea

Abstract

Hair growth cycles are mainly regulated by human dermal papilla cells (hDPCs) and human outer root sheath cells (hORSCs). Protecting hDPCs from excessive oxidative stress and hORSCs from glycogen phosphorylase (PYGL) is crucial to maintaining the hair growth phase, anagen. In this study, we developed a new PYGL inhibitor, hydroxytrimethylpyridinyl methylindolecarboxamide (HTPI) and assessed its potential to prevent hair loss. HTPI reduced oxidative damage, preventing cell death and restored decreased level of anagen marker ALP and its related genes induced by hydrogen peroxide in hDPCs. Moreover, HTPI inhibited glycogen degradation and induced cell survival under glucose starvation in hORSCs. In ex-vivo culture, HTPI significantly enhanced hair growth compared to the control with minoxidil showing comparable results. Overall, these findings suggest that HTPI has significant potential as a therapeutic agent for the prevention and treatment of hair loss.

Key Words: Hair loss, Dermal papillia cells, Outer root sheath cells, Anagen, Oxidative stress, Glycogen phosphorylase

INTRODUCTION

Hair follicles are multi-compartmented small organs that growth cycle goes through anagen, catagen, and telogen phase. The dermal portion of the hair follicle can be divided into two compartments, the dermal papilla and dermal sheath (Paus and Cotsarelis, 1999). Human Dermal Papilla Cells (hDPCs) and Human Outer Root Sheath Cells (hORSCs) are considered key cells particularly involved in skin development and hair growth and maintenance (Rajendran *et al*., 2022). The dermal papilla located at the base of the hair follicle, which responsible for hair follicle development from the epidermis and producing hair fibers (Elliott *et al*., 1999). Through their expression of growth-promoting signals, hDPCs play critical roles in regulating anagen initiation and the anagen to catagen transition (Yano *et al*., 2001). Additionally, hORSCs surround most hair follicle components and play important roles in supporting hDPCs and hair matrix cells (Choi *et al*., 2019).

Reactive oxygen species (ROS) are chemicals produced within cells and are associated with oxidative stress. Under physiological conditions, ROS act as a second messenger within the cell, carrying biological signals that control immune response, proliferation, metabolism, and differentiation of the cell (Koca *et al*., 2005; Bae *et al*., 2011). However, excessive ROS production can lead to cell damage and aging (Akar *et al*., 2002). It has been suggested that ROS are an important inducer of the androgen-dependent and -independent alopecia (Trüeb, 2009). Elevated ROS levels in hair follicle cells during the catagen phase facilitate hair follicle degeneration through the regulation of Trx1 and Foxp1 (Zhao *et al*., 2015). Balding scalps exhibits increased levels of ROS in the dermal papillae compared to non-balding scalps (Shin *et al*., 2013; Bakry *et al*., 2014). Moreover, elevated ROS levels are associated with decreased DPC motility (Bahta *et al*., 2008). In addition, DPCs from balding scalp also exhibits higher levels of cell senescence (Bahta *et al*., 2008). Recent research has

Open Access **https://doi.org/10.4062/biomolther.2024.098**

Received Jun 10, 2024 **Revised** Jul 5, 2024 **Accepted** Jul 17, 2024
Published Online Aug 6, 2024

***Corresponding Author**
E-mail: jshwang@khu.ac.kr
Tel: +82-31-201-3797, Fax: +82-31-204-2629
[†]The first two authors contributed equally to this work.

shown that hair loss caused by cisplatin is driven by ROS generation and ROS-induced apoptosis in dermal papilla cells (DPCs) (Luanpitpong *et al*., 2011).

The anagen phase is the longest and most active stage of the hair growth cycle. Because growing hair follicles (HF) have a high demand for energy and biosynthetic precursors produced by aerobic glycolysis, high levels of glycogen are required in hORSCs for cell division during the anagen phase (Choi *et al*., 2020; Figlak *et al*., 2021). In this context, hORSCs express enzymes for glycogen synthesis and metabolism, and can synthesize glycogen in the presence of lactate, indicating the operation of an internal Cori cycle (Figlak *et al*., 2021).

Glycogen phosphorylase (PYGL) is the enzyme that catalyzes glycogenolysis (Kowalik *et al*., 2017). It cleaves glucose by phosphorylating the non-reducing end of the glycogen polymer to form glucose-1-phosphate, which phosphoglucomutase then converts to glucose-6-phosphate (Kowalik *et al*., 2017). PYGL can regulate glucose supply in hORSCs by regulating the process of breaking down glycogen to produce glucose as needed (Figlak *et al*., 2021). It is well known that blocking PYGL considerably accelerates HF's *in vitro* growth and postpones the catagen phase's onset (Figlak *et al*., 2021).

We prepared a new PYGL inhibitor, the Compound named hydroxytrimethylpyridinyl methylindolecarboxamide (HTPI). This study verified whether HTPI can prevent hair loss by inhibiting ROS production which induces apoptosis in hDPCs. Additionally, we examined the effect of HTPI on PYGL, which regulates cellular glucose supply in hORSCs. In conclusion, HTPI exhibited a hair growth effect *ex vivo*. These studies can provide important information in preventing hair loss and can lay the foundation for the development of new treatment and prevention strategies.

MATERIALS AND METHODS

Reagents

In this study, the following reagents were used: water-soluble tetrazolium (WST) assay kit (EZ-cytox) from Daeil Lab service (Seoul, Korea); dimethyl sulfoxide (DMSO) from Biosesang (Seoul, Korea); hydrogen peroxide (H_2O_2), basic fibroblast growth factor (bFGF), insulin, hydrocortisone and glycogen assay kit from Sigma-Aldrich (St. Louis, MO, USA); lactate dehydrogenase (LDH) assay kit from Dojindo Molecular Technologies (Kumamoto, Japan); 5-(and-6)-carboxy-2',7'-dichlorofluorescein diacetate (DCFDA) and JC-1 dye from Abcam (Cambridge, UK); recombinant human DKK-1 protein from R&D Systems (Minneapolis, MN, USA); RNAiso Plus from Takara (Kusatsu, Japan); SYBR Green qPCR High-ROX PreMIX from Enzynomics (Daejeon, Korea); alkaline phosphatase staining assay from Biomax (Guri, Korea); collagen I, epilife medium and epilife defined growth supplement (EDGS) from Gibco (Grand Island, NY, USA); follicle dermal papilla cell growth medium and supplement mix from PromoCell (Heidelberg, Germany); Dulbecco's modified Eagle's medium (DMEM), fetal bovine serum (FBS), trypsin-EDTA, penicillin/streptomycin solution, Dulbecco's phosphate-buffered saline (DPBS) and phosphate-buffered saline (PBS) from WelGENE (Daegu, Korea). William's E medium, 2 mM L-glutamine, 10 U/mL penicillin, 100 ug/mL streptomycin and amphotericin B from Life Technologies (Carlsbad, CA, USA). Hydroxytrimethylpyridinyl Methylindolecarboxamide (HTPI) was dissolved in DMSO to the final concentration that did not exceed 0.1%.

Docking study

We utilized GNINA (version 1.1) (McNutt *et al*., 2021) for conducting protein-ligand docking, incorporating support for scoring and optimizing ligands through convolutional neural networks (CNN). The X-ray structure of the PYGL and ligand complex (PDB 2ZB2) was obtained from the RCSB Protein Data Bank. The protein was preprocessed using ProDy (Bakan *et al*., 2011) to eliminate non-protein components like water, cofactors, and ligands. The 3D structure of HTPI was formatted in SD using OpenBabel (O'Boyle *et al*., 2011). Subsequently, docking simulation was conducted with GNINA using the prepared protein and HTPI. The binding site was specified to the vicinity of the reference ligand which was extracted from the original PDB. Default settings were applied for all other parameters. The resulting binding poses were ranked based on CNNscore, which varies from 0 (poorest) to 1 (optimal). It should be noted that not a single but two identical ligand molecules are bound in the allosteric site. Therefore, docking was performed sequentially as follows.

(1) One ligand was removed from PDB 2ZB2 and the other ligand was left as is.

(2) HTPI was docked into the empty space resulting from the removal of one ligand in 2ZB2.

(3) The PDB resulting from docking now contains one 2ZB2 ligand and one HTPI molecule.

(4) The remaining 2ZB2 ligand was taken away from this PDB, while HTPI was left as is. This PDB was used for subsequent docking.

(5) HTPI was docked into the empty space resulting from the removal of 2ZB2 ligand.

(6) This docking result contains two HTPI molecules in the allosteric binding site.

Finally, we selected the most favorable binding mode by considering the CNN score and manually examining the binding interactions.

Cell culture

hDPCs and hORSCs were purchased by PromoCell. hDPCs were cultured in follicle dermal papilla cell growth medium supplemented with 4% fetal calf serum, 0.4% bovine pituitary extract, 1 ng/mL basic fibroblast growth factor (bFGF), and 5 μg/mL insulin (supplement mix) at 37°C incubator in a humidified atmosphere containing 5% CO_2. hORSCs were cultured in epilife medium supplemented with EDGS. Experiments utilized hDPCs and hORSCs from 3-5 passages. To induce oxidative stress with H_2O_2, serum deprivation was conducted by replacing the medium with fresh DMEM supplemented with 1% FBS and 1 ng/mL bFGF.

Cell viability

The proliferation of hDPCs was assessed using the WST kit (Daeil Lab service) following the manufacturer's instructions. hDPCs (5.0×10^3 cells/well) were seeded in 96-well plates and incubated overnight. Subsequently, the medium was replaced with fresh DMEM supplemented with 1% FBS and 1 ng/mL bFGF for 24 h. hDPCs were pre-incubated with HTPI for 2 h and treated with H_2O_2 for 24 h. The medium was replaced with a medium containing 10% WST dye, and the cells were then incubated in an incubator at 37°C and 5% CO_2 for 1 h. Absorbance was measured at 450 nm using a microplate reader

(Tecan, Mannedorf, Switzerland).

Lactate dehydrogenase assay

Cytotoxicity was determined by Cytotoxicity LDH assay kit (Dojindo Molecular Technologies) according to manufacturer's instructions. hDPCs (5.0×10^3 cells/well) were pre-incubated with DMEM medium containing 1% FBS for 24 h. The cells were treated with H_2O_2 for 24 h. After replacing with the working solution, the samples were protected from light and incubated at room temperature. After 30 min, stop solution was added. The absorbance was measured at 490 nm by Tecan microplate reader.

Intercellular ROS assay

The intracellular ROS level was assessed using the DCF-DA method (Abcam). hDPCs (5.0×10^3 cells/well) were seeded in 96-well black plates and incubated for 24 h. The medium was then replaced with fresh serum-starvation medium and incubated overnight. Cells were pre-treated with HTPI for 2 h and stained with the DCF-DA probe. After 45 min, cells were treated H_2O_2 with DMEM without phenol-red for 4 h. Fluorescent intensity was measured at Ex/Em=485/535 nm.

JC-1 staining

JC-1 staining was examined using JC-1 staining kit (Abcam) following the manufacturer's protocols. hDPCs (5.0×10^3 cells/well) were seeded in 96-well black plates. Cells were pre-treated with HTPI for 2 h and stained with JC-1 dye. After 10 min, cells were treated H_2O_2 with DMEM without phenol-red for 2 h. Fluorescent intensity was measured at Ex/Em=475/590 nm using Tecan microplate reader.

ALP staining

hDPCs (1.5×10^5 cells/well) were seeded in 6-well plates for 24 h prior to be stimulated with HTPI. The cells were treated with H_2O_2 in the absence or presence of HTPI for 24 h. For ALP staining (Vector Laboratories, CA, USA), cells were washed with cold PBS and homogenized. The cell lysate was centrifuged at 15,000xg for 20 min to obtain the supernatant. The supernatant was incubated with 5 mM *p*NPP at 37°C for 1 h and the reaction was stopped by adding stop solution. The absorbance was measured at 405 nm by Tecan.

Glycogen assay

The concentration of glycogen in hORSCs was determined using a glycogen assay kit (Sigma-Aldrich) following the manufacturer's protocols. Briefly, hORSCs (1.5×10^5 cells/well) were seeded in 6-well plate for 24 h. To induce glucose starvation, DMEM without glucose but supplemented with 55 mg/L pyruvate was utilized. HTPI was treated for 2 h before glucose starvation. After starvation, the cells were homogenized and lysed. The lysate was centrifuged, and the supernatant was transferred into tubes for quantification. Glycogen was degraded to glucose using a hydrolysis enzyme mix and then developed with a colorimetric development enzyme mix which produces a colorimetric 570 nm.

Quantitative Real-time PCR

hDPCs (1.5×10^5 cells/well) were seeded in 6-well plates and cultured for 24 h. After overnight serum limitation, HTPI was pre-treated. After 2 h, cells were treated with H_2O_2 in present of rhDKK-1. Total RNA was extracted with RNAiso Plus (Takara, Shiaga, Japan). Reverse transcription was then performed with oligo-primers to obtain cDNA. Finally, qPCR analysis was accomplished on a CFX Connect Real-Time PCR Detection System (Bio-Rad, Hercules, CA, USA) using SYBR Green qPCR High-ROX PreMIX.

Human hair follicle organ culture

Human scalp skin was obtained from nonbalding areas from patients undergoing hair transplant surgery with written consent and approval by the Institutional Review Board of Dankook University Hospital (IRB no. DKUH. 2021-12-005). Human hair follicles were isolated by microdissection under the microscope. Anagen VI hair follicles were chosen for the study. Each treatment group consist of 6 hair follicles and the experiments repeated 3 times. Isolated hair follicles were maintained in William's E medium supplemented with 10 μg/mL insulin, 10 ng/mL hydrocortisone, 2 mM L-glutamine, and 10 U/mL penicillin, 100 μg/mL streptomycin, and 25 μg/mL amphotericin B. All cultures were incubated at 37°C in an atmosphere of 5% CO_2 and 95% air.

Statistical analysis

Statistical analysis of data was performed with the ANOVA test and Mann-Whitney U test using the Statistical Packages for Social Sciences (SPSS) program (SPSS, Inc., Chicago, IL, USA).

RESULTS

Docking study of HTPI to the PYGL allosteric site

PYGL spontaneously forms an active dimer when two identical subunits are in the activated state (Oikonomakos *et al*., 2000). It is regulated primarily through reversible phosphorylation and allosteric effectors such as AMP, glucose-1-phosphate and glycogen as activators and ATP, glucose-6-phosphate and glucose as inhibitors (Rocha *et al*., 2021). But the recently identified allosteric site is located at the dimeric interface and differs from the previously known allosteric sites where aforementioned allosteric effectors bind. PYGL can be allosterically inhibited by binding of ligands to this new allosteric site (Onda *et al*., 2008). This paper describes the discovery of a series of allosteric inhibitors of PYGL and the crystal structure (PDB 2ZB2) of the representative compound. We used the PDB 2ZB2 for docking study of HTPI. Docking of HTPI into PYGL was proceeded as described in the METHOD section. Two HTPI molecules are bound in the allosteric site formed at the dimeric interface of two PYGL monomers (Fig. 1). The binding interactions between PYGL and HTPI are depicted (Fig. 2). The amide nitrogen of HTPI forms a hydrogen bond to the carbonyl oxygen of Thr38. The indole and pyridine rings of the ligand have a cation-p interaction with the guanidyl group of Arg60 and a p-p stacking interaction with the aromatic ring of His57, respectively.

HTPI prevented H_2O_2-induced cell death in hDPCs

Based on the role of HFDPC in hair follicles, we first evaluated the cell viability of hDPCs following exposure to different concentrations of HTPI (0.01-100 μM). According to the cell viability analysis results, HTPI induced toxicity in hDPCs at a concentration of 100 μM for 24 h (Fig. 3A). Under conditions of oxidative stress, hDPCs were observed to undergo premature

senescence (Upton *et al*., 2015; Huang *et al*., 2017). In this study, H_2O_2 was used as the oxidative stress inducer, resulting in a concentration-dependent reduction in the viability of cultured hDPCs (data not shown). While H_2O_2 reduced cell viability by approximately 30% and 50% at concentrations of 750 μM and 1000 μM, respectively, the decrease in cell viability induced by H_2O_2 was restored after pre-treatment with HTPI for 2 h in a concentration-dependent manner (Fig. 3B). Also, LDH assay showed that H_2O_2 increased cell cytotoxicity but HTPI treatment resulted in a reduction in cytotoxicity levels (Fig. 3C). We have found that HTPI decreased ROS-induced cell cytotoxicity and the LDH activities.

HTPI protected cultured hDPCs from H_2O_2-induced oxidative stress in hDPCs

As mentioned earlier, ROS are one of the major contributors to hair loss. There is increasing evidence that removal of ROS promotes hair follicle regeneration (Le Thi *et al*., 2020). To determine whether HTPI protect hDPCs from ROS, we conducted DCFDA assay to assess intercellular ROS changes. H_2O_2 was used to induce ROS production. The pretreatment of HTPI at 0.5 μM significantly reduced the increased ROS production induced by H_2O_2 (Fig. 4A). We also analyzed mitochondrial ROS production using JC-1 assay. Compared with the control group, H_2O_2 treatment showed decreased JC-1 aggregates/monomer ratio, indicating that the mitochondrial membrane potential was decreased. HTPI increased JC-1 aggregates/monomer ratio ranged about 10% but with significance at 750 μM H_2O_2 (Fig. 4B).

HTPI restored the decreased alkaline phosphatase activity level by H_2O_2 in hDPCs

Alkaline phosphatase (ALP), an important regulator of energy metabolism, was identified as a critical anagen marker (Iida *et al*., 2007). ALP activity is associated with the hair-inducing capability of hDPCs and the decrease in ALP activity is related to the transition from the anagen phase to the catagen phase (Rendl *et al*., 2008; Woo *et al*., 2012). It was found that the ALP activity level decreased by approximately 50% following H_2O_2 treatment but HTPI restored the ALP activity level in a concentration dependent manner with statistical significance (Fig. 5). Our data suggest that HTPI could inhibit the ROS-induced catagen progression via increasing the ALP activity. Furthermore, HTPI regulated the mRNA expression levels of anagen and catagen markers (Supplementary Fig. 1A, 1B). The decreased expression of the anagen marker, β-catenin, upon hydrogen peroxide treatment was restored by HTPI. Additionally, DKK-1, a catagen marker, decreased upon treatment with HTPI alone and attenuated the increased levels of DKK-1 induced by H_2O_2. This suggests that prolonging the anagen phase and preventing progression to catagen in hDPCs can prevent hair loss.

HTPI regulated glycogen degradation in hORSCs

Glucose serves as a crucial fuel to sustain hair growth and a primary precursor for glycogen synthesis (Williams *et al*., 1993). Therefore, we investigated whether glycogen storage is depleted by glucose starvation and HTPI regulates glycogen breakdown in hORSCs. Quantitative glycogen assay showed that glycogen contents in hORSCs cultured in a glucose-free medium were markedly reduced. However, HTPI

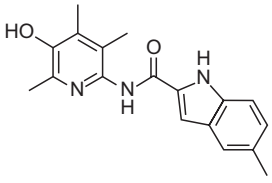

Fig. 1. The chemical structure of HTPI.

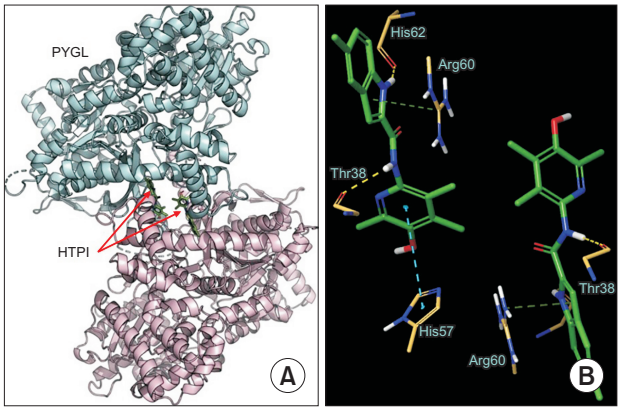

Fig. 2. Predicted binding mode of PYGL and HTPI complex. (A) Two identical subunits of PYGL are depicted in pale cyan and pink colors. Two HTPI molecules are bound allosterically at the dimeric interface of PYGL and are depicted as sticks in green. (B) Major binding interactions in the PYGL and HTPI complex. Hydrogen bonds, cation-p and p-p stacking interactions are shown as dotted lines in yellow, green and cyan colors, respectively.

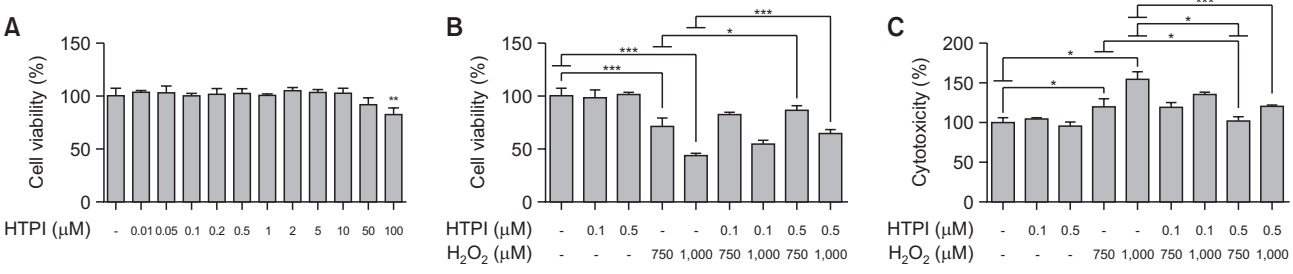

Fig. 3. hDPCs viability in the presence of various concentrations of HTPI. (A) HTPI was treated with hDPCs for 24 h. (B, C) HTPI was pretreated for 2 h in hDPCs and treated with H_2O_2 for 24 h. *p<0.05; **p<0.01; ***p<0.001 vs. control.

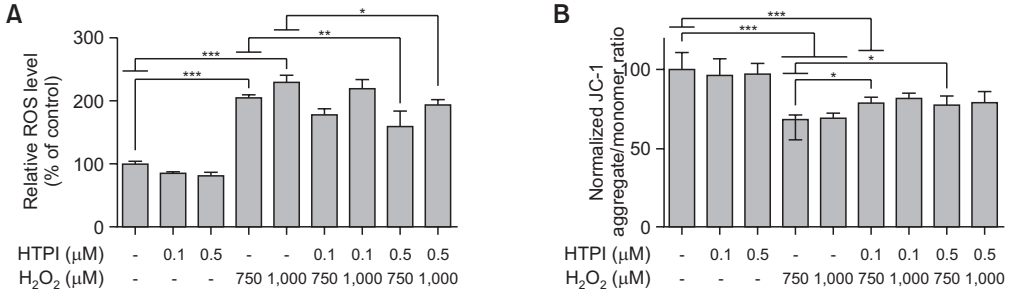

Fig. 4. HTPI reduces ROS levels induced by H_2O_2. The ROS production of hDPCs was measured. (A) Intracellular ROS content was measured after HTPI pre-treatment for 2 h and H_2O_2 treatment for 4 h using DCFDA. (B) Mitochondrial ROS production was analyzed using the JC-1 assay. *p<0.05; **p<0.01; ***p<0.001 vs. control.

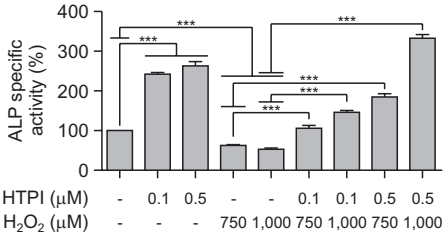

Fig. 5. HTPI increased the level of ALP activity, which was reduced by H_2O_2 treatment in hDPCs. After pre-treatment with HTPI for 2 h, hDPCs were treated with H_2O for 24 h. ***p<0.001 vs. control.

inhibited glycogen degradation in a dose-dependent manner (Fig. 6A). It is known that glycogen content markedly decreases during the catagen phase (Figlak *et al*., 2021). This result indicates that HTPI could prolong anagen phase and inhibit catagen transition as the crucial glycogen metabolism enzyme in hORSCs. Also, HTPI increased the decreased cell viability induced by glucose starvation (Fig. 6B). Moreover, pretreatment with HTPI prevented cell death in hORSCs induced by DKK-1 protein (Supplementary Fig. 2).

HTPI promoted human hair growth ex vivo

The effect of HTPI on human hair growth was investigated in human hair follicle organ culture model. HTPI significantly increased the hair growth compared with non-treated control (Fig. 7). On day 8 of culture, HTPI increased the length of hair shaft by 10.5% (1 μM) and 11.1% (2 μM) compared with non-treated control. A positive control minoxidil showed a comparable result.

DISCUSSION

Hair fulfills diverse vital physiological roles, encompassing the dispersion of sweat-gland secretions, including pheromones, and furnishing protection against environmental elements (Paus and Cotsarelis, 1999). The reciprocal interaction between mesenchymal dermal papilla and the follicular epithelium is necessary for the physiological growth and cyclical processes of hair follicles (Hardy, 1992; Chuong, 1998). Notably, hDPCs act as secondary germ cells localized in the hair-follicle bulge to instigate the renewal of the lower follicular segment at the onset of each successive follicular cycle (Cotsarelis *et al*., 1990). hDPCs orchestrate the proliferation and maturation of hair follicles, directing the proliferation, migration, and differentiation of surrounding matrix cells into the emerging hair shaft (Driskell *et al*., 2011). Furthermore, the dynamics of hair size, morphology, and cycling are intricately regulated by the abundance of hDPCs (Chi *et al*., 2013). Our findings elucidate that pretreatment with HTPI reduced the heightened ROS production induced by H_2O_2 and effectively mitigates H_2O_2-triggered orchestrate cell death in hDPCs.

The conspicuous expression of alkaline phosphatase (ALP) activity by follicular dermal papilla during and post development is a widely acknowledged phenomenon (Hardy, 1952). This enzymatic activity has been utilized as a valuable indicator to delineate the spatial distribution, morphology, and dimensions of dermal papilla within cutaneous samples (Handjiski *et al*., 1994; Müller-Röver *et al*., 2001). Studies have demonstrated that early-passage dermal papilla cells exhibiting elevated ALP levels possess the capacity to instigate hair follicle neogenesis upon engraftment into cutaneous wounds (McElwee *et al*., 2003). Conversely, dermal papilla cells in late passages exhibit diminished ALP activity and are inept at inducing hair follicle regeneration (McElwee *et al*., 2003). Our findings demonstrate that HTPI could inhibit the ROS-induced catagen progression via increasing the ALP activity.

The hair follicle (HF) features a distinctive energetic mechanism, known as the Cori cycle, which relies on glycogen reserves (Figlak *et al*., 2021). Earlier investigations have documented the presence of glycogen within the outer root sheath (ORS) of hair follicles in both human and murine specimens (Montagna *et al*., 1951; Shipman *et al*., 1955; ELLIS and Montagna, 1958). Considering the role of PYGL in glycogen breakdown, glycogen metabolism assumes significance in initiating the catagen phase, potentially furnishing the requisite energy for apoptotic processes (Figlak *et al*., 2021). Notably, hORSCs emerge as pivotal sites for glycogen synthesis, functioning as active repositories for glycogen storage while also demonstrating gluconeogenic capabilities. Fijlak *et al*. elucidated that inhibition of PYGL leads to a notable reduction in the number of hair follicles transitioning into the catagen phase, thereby prolonging the anagen stage (Figlak *et al*., 2021). Our investigation underscores the efficacy of HTPI in extending the anagen phase and impeding the onset of catagen transition by targeting crucial glycogen metabolism enzymes within hORSCs.

Recent progress in understanding of the biology and pa-

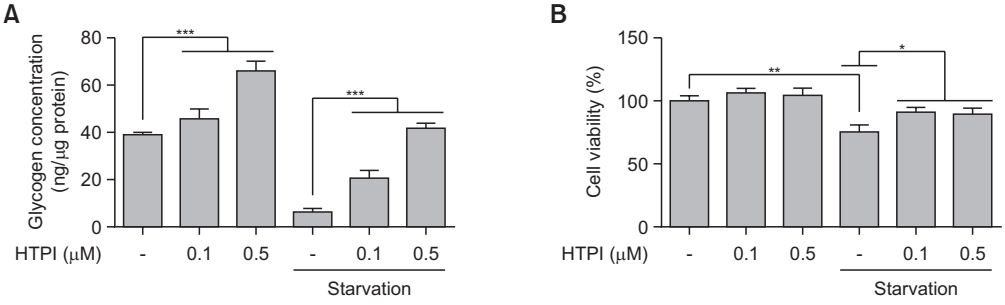

Fig. 6. Effect of HTPI on hORSCs in the presence or absence of glucose. hORSCs were pre-treated with HTPI for 2 h, and then hORSCs were incubated with glucose-free medium for 24 h. (A) Glycogen in hORSCs. (B) Cell viability was measured. **p*<0.05; ***p*<0.01; ****p*<0.001 vs. control.

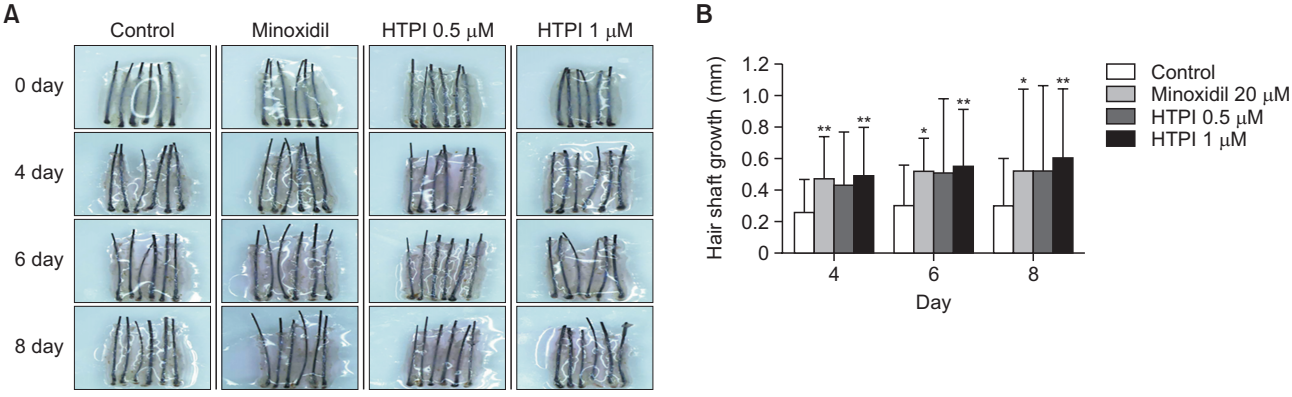

Fig. 7. Effect of HTPI on hair growth in human hair follicle organ culture. In order to evaluate the effect of HTPI, the anagen human hair follicle were prepared and cultured for 8 days. HTPI was treated at concentrations of 1 and 2 μM. (A) At day 4, 6 and 8, the cultured hair follicles were photo-documented. (B) The hair shaft growth was analyzed. Minoxidil was used as a positive control. The data represent the mean±SD of eighteen follicles. *p*-values were obtained by Mann-Whitney U test. Significantly different compared with control. **p*<0.05; ***p*<0.01 vs. control.

thology of hair follicles should lead to more effective therapies for disorders of hair growth.[1] All of the study's findings point to the various impacts that HTPI has on hDPCs and hORSCs, including the regulation of cell proliferation, defense against oxidative stress, stimulation of metabolic processes, and relief of growth inhibition caused by glucose shortage. These findings indicate a possible therapeutic use of HTPI in prolonging the anagen phase of hair follicles and preventing oxidative damage. Ultimately, we confirmed the hair growth-promoting ability of HTPI using an ex-vivo model. HTPI's effectiveness is comparable to that of minoxidil, a well-established hair growth stimulant used as a positive control in this study. These findings support the potential of HTPI as a significant hair growth stimulant. We also point to directions for future study into the drug's mechanism of action and prospective applications in the treatment of hair-related conditions or regenerative medicine.

REFERENCES

Akar, A., Arca, E., Erbil, H., Akay, C., Sayal, A. and Gür, A. R. (2002) Antioxidant enzymes and lipid peroxidation in the scalp of patients with alopecia areata. *J. Dermatol. Sci.* **29**, 85-90.

Bae, Y. S., Oh, H., Rhee, S. G. and Do Yoo, Y. (2011) Regulation of reactive oxygen species generation in cell signaling. *Mol. Cells* **32**, 491-509.

Bahta, A. W., Farjo, N., Farjo, B. and Philpott, M. P. (2008) Premature senescence of balding dermal papilla cells *in vitro* is associated with p16INK4a expression. *J. Invest. Dermatol.* **128**, 1088-1094.

Bakan, A., Meireles, L. M. and Bahar, I. (2011) ProDy: protein dynamics inferred from theory and experiments. *Bioinformatics (Oxford, England)* **27**, 1575-1577.

Bakry, O. A., Elshazly, R. M. A., Shoeib, M. A. M. and Gooda, A. (2014) Oxidative stress in alopecia areata: a case-control study. *Am. J. Clin. Dermatol.* **15**, 57-64.

Chi, W., Wu, E. and Morgan, B. A. (2013) Dermal papilla cell number specifies hair size, shape and cycling and its reduction causes follicular decline. *Development* **140**, 1676-1683.

Choi, M., Choi, S. J., Jang, S., Choi, H. I., Kang, B. M., Hwang, S. T. and Kwon, O. (2019) Shikimic acid, a mannose bioisostere, promotes hair growth with the induction of anagen hair cycle. *Sci. Rep.* **9**, 17008.

Choi, M., Choi, Y. M., Choi, S. Y., An, I. S., Bae, S., An, S. and Jung, J. H. (2020) Glucose metabolism regulates expression of hair-inductive genes of dermal papilla spheres via histone acetylation. *Sci. Rep.* **10**, 4887.

Chuong, C. M. (1998) Molecular Basis of Epithelial Appendage Morphogenesis (Vol. 1). Landes Bioscience.

Cotsarelis, G., Sun, T. T. and Lavker, R. M. (1990) Label-retaining cells reside in the bulge area of pilosebaceous unit: implications for follicular stem cells, hair cycle, and skin carcinogenesis. *Cell* **61**, 1329-1337.

Driskell, R. R., Clavel, C., Rendl, M. and Watt, F. M. (2011) Hair follicle

dermal papilla cells at a glance. *J. Cell Sci.* **124**, 1179-1182.
Elliott, K., Messenger, A. G. and Stephenson, T. J. (1999) Differences in hair follicle dermal papilla volume are due to extracellular matrix volume and cell number: implications for the control of hair follicle size and androgen responses. *J. Invest. Dermatol.* **113**, 873-877.
Ellis, R. A. and Montagna, W. (1958) Histology and cytochemistry of human skin. XV. Sites of phosphorylase and amylo-1, 6-glucosidase activity. *J. Histochem. Cytochem.* **6**, 201-207.
Figlak, K., Williams, G., Bertolini, M., Paus, R. and Philpott, M. P. (2021) Human hair follicles operate an internal Cori cycle and modulate their growth via glycogen phosphorylase. *Sci. Rep.* **11**, 20761.
Handjiski, B. K., Eichmüller, S., Hofmann, U., Czarnetzki, B. M. and Paus, R. (1994) Alkaline phosphatase activity and localization during the murine hair cycle. *Br. J. Dermatol.* **131**, 303-310.
Hardy, M. H. (1952) The histochemistry of hair follicles in the mouse. *Am. J. Anat.* **90**, 285-337.
Hardy, M. H. (1992) The secret life of the hair follicle. *Trends Genet.* **8**, 55-61.
Huang, W. Y., Huang, Y. C., Huang, K. S., Chan, C. C., Chiu, H. Y., Tsai, R. Y. Chan, J. Y. and Lin, S. J. (2017) Stress-induced premature senescence of dermal papilla cells compromises hair follicle epithelial-mesenchymal interaction. *J. Dermatol. Sci.* **86**, 114-122.
Iida, M., Ihara, S. and Matsuzaki, T. (2007) Hair cycle-dependent changes of alkaline phosphatase activity in the mesenchyme and epithelium in mouse vibrissal follicles. *Dev. Growth Differ.* **49**, 185-195.
Koca, R., Armutcu, F., Altinyazar, H. C. and Gürel, A. (2005) Evaluation of lipid peroxidation, oxidant/antioxidant status, and serum nitric oxide levels in alopecia areata. *Med. Sci. Monit.* **11**, CR296-CR299.
Kowalik, M. A., Columbano, A. and Perra, A. (2017) Emerging role of the pentose phosphate pathway in hepatocellular carcinoma. *Front. Oncol.* **7**, 87.
Le Thi, P., Lee, Y., Tran, D. L., Thi, T. T. H., Kang, J. I., Park, K. M. and Park, K. D. (2020) In situ forming and reactive oxygen species-scavenging gelatin hydrogels for enhancing wound healing efficacy. *Acta Biomater.* **103**, 142-152.
Luanpitpong, S., Nimmannit, U., Chanvorachote, P., Leonard, S. S., Pongrakhananon, V., Wang, L. and Rojanasakul, Y. (2011) Hydroxyl radical mediates cisplatin-induced apoptosis in human hair follicle dermal papilla cells and keratinocytes through Bcl-2-dependent mechanism. *Apoptosis* **16**, 769-782.
McElwee, K. J., Kissling, S., Wenzel, E., Huth, A. and Hoffmann, R. (2003) Cultured peribulbar dermal sheath cells can induce hair follicle development and contribute to the dermal sheath and dermal papilla. *J. Invest. Dermatol.* **121**, 1267-1275.
McNutt, A. T., Francoeur, P., Aggarwal, R., Masuda, T., Meli, R., Ragoza, M., Sunseri, J. and Koes, D. R. (2021) GNINA 1.0: molecular docking with deep learning. *J. Cheminform.* **13**, 43.
Montagna, W., Chase, H. B. and Hamilton, J. B. (1951) The distribution of glycogen and lipids in human skin. *J. Invest. Dermatol.* **17**, 147-157.
Müller-Röver, S., Handjiski, B., van der Veen, C., Eichmüller, S., Foitzik, K., McKay, I. A., Stenn, K. S. and Paus, R. (2001) A comprehensive guide for the accurate classification of murine hair follicles in distinct hair cycle stages. *J. Invest. Dermatol.* **117**, 3-15.
O'Boyle, N. M., Banck, M., James, C. A., Morley, C., Vandermeersch, T. and Hutchison, G. R. (2011) Open Babel: an open chemical toolbox. *J. Cheminform.* **3**, 33.
Oikonomakos, N. G., Skamnaki, V. T., Tsitsanou, K. E., Gavalas, N. G. and Johnson, L. N. (2000) A new allosteric site in glycogen phosphorylase b as a target for drug interactions. *Structure* **8**, 575-584.
Onda, K., Suzuki, T., Shiraki, R., Yonetoku, Y., Negoro, K., Momose, K., Katayama, N., Orita, M., Yamaguchi, T., Ohta, M. and Tsukamoto, S. (2008) Synthesis of 5-chloro-N-aryl-1H-indole-2-carboxamide derivatives as inhibitors of human liver glycogen phosphorylase a. *Bioorg. Med. Chem.* **16**, 5452-5464.
Paus, R. and Cotsarelis, G. (1999) The biology of hair follicles. *N. Engl. J. Med.* **341**, 491-497.
Rajendran, R. L., Gangadaran, P., Kwack, M. H., Oh, J. M., Hong, C. M., Sung, Y. K., Lee, J. and Ahn, B. C. (2022) Application of extracellular vesicles from mesenchymal stem cells promotes hair growth by regulating human dermal cells and follicles. *World J. Stem Cells* **14**, 527-538.
Rendl, M., Polak, L. and Fuchs, E. (2008) BMP signaling in dermal papilla cells is required for their hair follicle-inductive properties. *Genes Dev.* **22**, 543-557.
Rocha, S., Lucas, M., Araújo, A. N., Corvo, M. L., Fernandes, E. and Freitas, M. (2021) Optimization and validation of an *in vitro* standardized glycogen phosphorylase activity assay. *Molecules* **26**, 4635.
Shin, H., Yoo, H. G., Inui, S., Itami, S., Kim, I. G., Cho, A. R., Lee, D. H., Park, W. S., Kwon, O., Cho, K. H. and Won, C. H. (2013) Induction of transforming growth factor-beta 1 by androgen is mediated by reactive oxygen species in hair follicle dermal papilla cells. *BMB Rep.* **46**, 460-464.
Shipman, M., Chase, H. B. and Montagna, W. (1955) Glycogen in skin of the mouse during cycles of hair growth. *Proc. Soc. Exp. Biol. Med.* **88**, 449-451.
Trüeb, R. M. (2009) Oxidative stress in ageing of hair. *Int. J. Trichology* **1**, 6-14.
Upton, J. H., Hannen, R. F., Bahta, A. W., Farjo, N., Farjo, B. and Philpott, M. P. (2015) Oxidative stress–associated senescence in dermal papilla cells of men with androgenetic alopecia. *J. Invest. Dermatol.* **135**, 1244-1252.
Williams, R., Philpott, M. P. and Kealey, T. (1993) Metabolism of freshly isolated human hair follicles capable of hair elongation: a glutaminolytic, aerobic glycolytic tissue. *J. Invest. Dermatol.* **100**, 834-840.
Woo, W. M., Zhen, H. H. and Oro, A. E. (2012) Shh maintains dermal papilla identity and hair morphogenesis via a Noggin–Shh regulatory loop. *Genes Dev.* **26**, 1235-1246.
Yano, K., Brown, L. F. and Detmar, M. (2001) Control of hair growth and follicle size by VEGF-mediated angiogenesis. *J. Clin. Invest.* **107**, 409-417.
Zhao, J., Li, H., Zhou, R., Ma, G., Dekker, J. D., Tucker, H. O., Yao, Z. and Guo, X. (2015) Foxp1 regulates the proliferation of hair follicle stem cells in response to oxidative stress during hair cycling. *PLoS One* **10**, e0131674.